Multiscale modelling of polycrystalline UO2: full-field simulations (FFT) and model reduction technique (NTFA)

Julien Labat, Rodrigue Largenton, Jean-Claude Michel, Bruno Michel

Multiscale Modelling of Polycrystalline UO_2: Full-Field Simulations (FFT) and Model Reduction Technique (NTFA)

J. LABAT[1,2], R. LARGENTON[1], J.-C. MICHEL[2], B. MICHEL[3]

[1] *MMC, EDF R&D, F-77818 Moret-sur-Loing Cedex, France*
E-mail: julien.labat@edf.fr, rodrigue.largenton@edf.fr
[2] *Aix Marseille Univ, CNRS, Centrale Marseille, LMA UMR 7031, Marseille, France*
E-mail: michel@lma.cnrs-mrs.fr
[3] *CEA, DES/IRESNE/DEC/SESC/LSC, Saint-Paul-lez-Durance, 13108, France*
E-mail: bruno.michel@cea.fr

Industrial Context

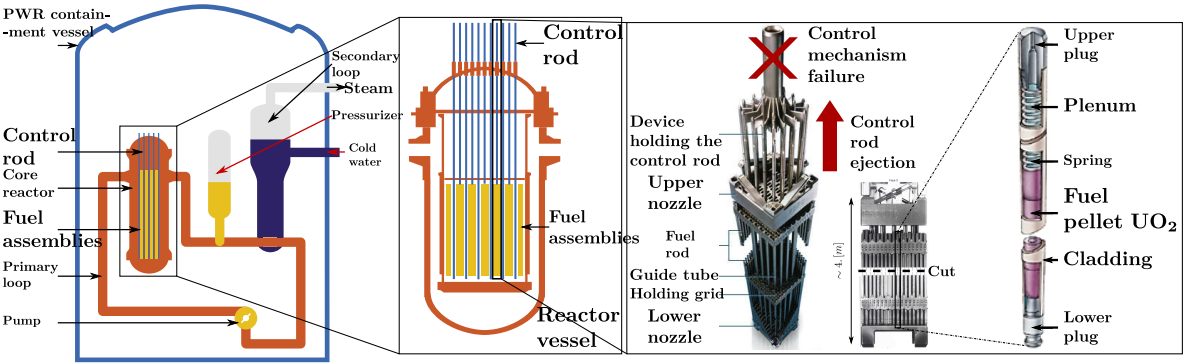

RIA - Reactivity Initiated Accident (Class 4)

◇ **Specific thermo-mechanical loading**:

- ▶ $T \in [1000,\ 2600]\ [°C]$
- ▶ $\dot{\varepsilon} \in [10^{-6},\ 10^{-1}]\ [s]^{-1}$

Behaviour law of UO_2 is highly dependent on the loading conditions $(T, \dot{\varepsilon})$

Method

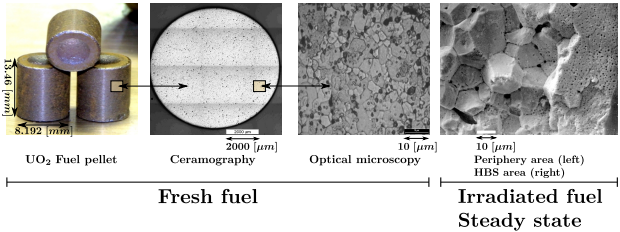

Scale of the UO_2 pellet

◇ Non uniform Transformation Field Analysis (NTFA) model at each integration point

◇ Access to the local fields

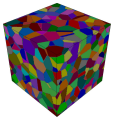

Polycrystal: 500 Grains

Scale of a single crystal

◇ 1 Grain ($\sim 10\,[\mu m]$)

◇ Elasto viscoplastic behaviour law with isotropic strain hardening

Model reduction: NTFA

Scale of a polycrystal: RVE

◇ ~ 500 Grains (500 single crystals).

◇ **Full Field simulation: FFT**

◇ Strain incompatibilities

Inverse calibration

Experimental Results

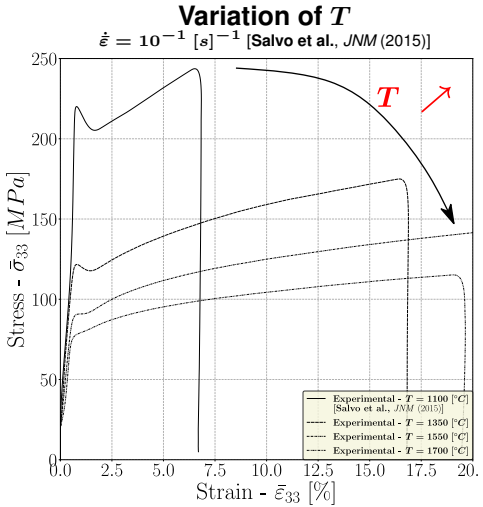

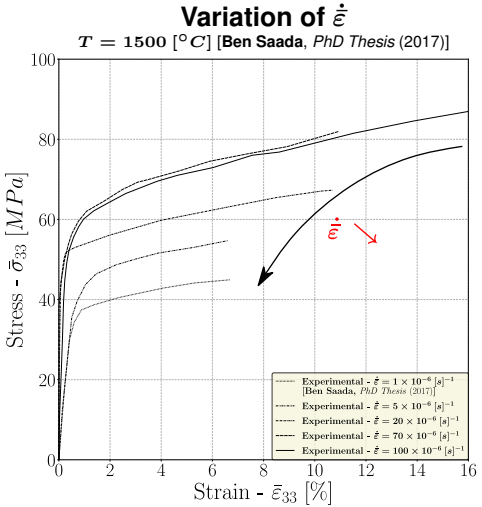

Inverse Calibration Process

Aim: to recover the asymptotic behaviour for all loading conditions

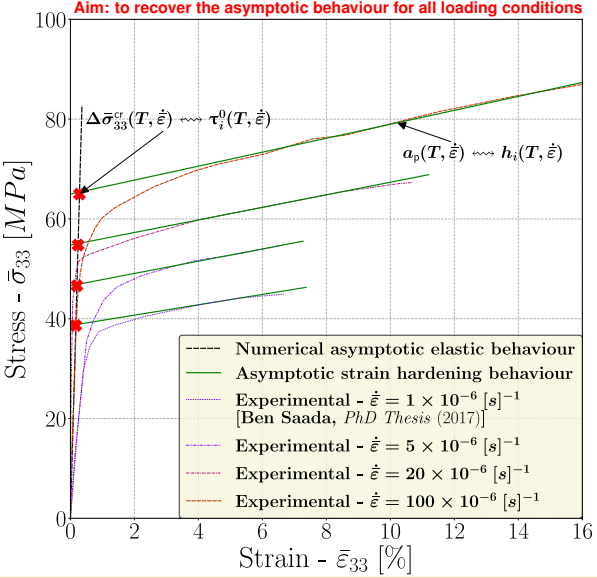

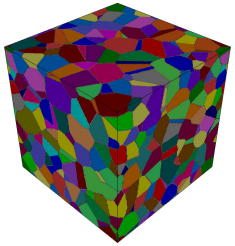

Calculation of $(\Delta\bar{\sigma}^{cr}_{33}, a_p)$ linked to the local parameters (τ^0_i, h_i)

$$\dot{\gamma}^{vp}_s = \dot{\gamma}^0_i \times \left(\frac{|\tau_s|}{r_i}\right)^{n_i} \times sgn(\tau_s),$$

$$r_i(\boldsymbol{x},t) = \tau^0_i(T,\dot{\bar{\varepsilon}}) + h_i(T,\dot{\bar{\varepsilon}}) \times p_i(\boldsymbol{x},t),$$

$$\dot{p}_i = \sum_{s\in S_i} \dot{\gamma}^p_s,\ \dot{\gamma}^p_s = |\dot{\gamma}^{vp}_s|, \qquad (1)$$

with:
- $\dot{\gamma}^{vp}_s$ evolution law inspired by **[Knezevic et al.**, *IJP* (2013)],
- $(\boldsymbol{\tau^0_i}, \boldsymbol{h_i})(T,\dot{\bar{\varepsilon}})$ functions to be calibrated.

Table of contents

Single Crystal Scale: Elasto Viscoplastic Behaviour with Isotropic Strain Hardening

$$w\left(\boldsymbol{\varepsilon},\boldsymbol{\varepsilon}_{\mathsf{vp}},p\right)=\frac{1}{2}\left(\boldsymbol{\varepsilon}-\boldsymbol{\varepsilon}_{\mathsf{vp}}\right):\boldsymbol{L}:\left(\boldsymbol{\varepsilon}-\boldsymbol{\varepsilon}_{\mathsf{vp}}\right)+w^{\mathsf{iso}}(p),\ \boldsymbol{\sigma}=\frac{\partial w}{\partial\boldsymbol{\varepsilon}}\left(\boldsymbol{\varepsilon},\boldsymbol{\varepsilon}_{\mathsf{vp}},p\right),$$

with: w local free-energy,

$$\boldsymbol{\varepsilon}(\boldsymbol{x},t)=\boldsymbol{\varepsilon}_{\mathsf{e}}(\boldsymbol{x},t)+\boldsymbol{\varepsilon}_{\mathsf{vp}}(\boldsymbol{x},t),\ \boldsymbol{\varepsilon}_{\mathsf{vp}}(\boldsymbol{x},t)=\sum_{s}\gamma_{s}^{\mathsf{vp}}(\boldsymbol{x},t)\ \boldsymbol{m_s}(\boldsymbol{x}),$$

with:
- $\boldsymbol{m_s}$ Schmid tensor UO_2 fluorite crystallographic structure [**Soulacroix**, *PhD Thesis* (2014)],
- γ_s^{vp} slip on the considered system (s).

(2)

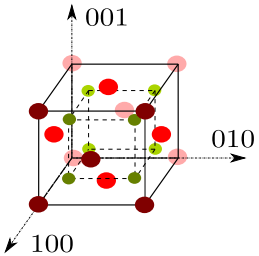

Fluorite crystallographic structure: oxygen atoms in red, uranium atoms in green

$$\psi_{\mathsf{vp}}=\sum_{s}\psi_{\mathsf{vp},s},\ \psi_{\mathsf{vp},s}(\boldsymbol{\mathcal{A}}_{\mathsf{vp}},\mathcal{A}_{\mathsf{p},i})=\dot{\gamma}_i^0\times\frac{-\mathcal{A}_{\mathsf{p},i}}{n_i+1}\times\left(\frac{|\mathcal{A}_{\mathsf{vp},s}|}{-\mathcal{A}_{\mathsf{p},i}}\right)^{n_i+1},$$

$$\psi_{\mathsf{p}}=\sum_{s}\psi_{\mathsf{p},s},\quad\psi_{\mathsf{p},s}(\boldsymbol{\mathcal{A}}_{\mathsf{vp}},\mathcal{A}_{\mathsf{p},i})=\dot{\gamma}_i^0\times\frac{|\mathcal{A}_{\mathsf{vp},s}|}{(n_i-1)}\times\left(\frac{|\mathcal{A}_{\mathsf{vp},s}|}{-\mathcal{A}_{\mathsf{p},i}}\right)^{n_i-1},$$

with:
- $(\psi_{\mathsf{vp}},\psi_{\mathsf{p}})$ dissipation potentials $\rightsquigarrow(\dot{\boldsymbol{\varepsilon}}_{\mathsf{vp}},\dot{p})$,
- $(\boldsymbol{\mathcal{A}}_{\mathsf{vp}},\mathcal{A}_{\mathsf{p},i})$ thermodynamic forces $\longleftrightarrow(\boldsymbol{\varepsilon}_{\mathsf{vp}},p_i)$.

Local Problem to be Solved for RVE V : Equation System (3) *Coupled with Evolution Laws* (4)

$$\left.\begin{array}{l} \boldsymbol{\sigma}(\boldsymbol{x},t) = \boldsymbol{L}(\boldsymbol{x}) : (\boldsymbol{\varepsilon}(\boldsymbol{x},t) - \boldsymbol{\varepsilon}_{\mathsf{vp}}(\boldsymbol{x},t)), \quad \boldsymbol{\varepsilon}_{\mathsf{vp}}(\boldsymbol{x},t) = \sum_s \gamma_s^{\mathsf{vp}}(\boldsymbol{x},t)\, \boldsymbol{m_s}(\boldsymbol{x}), \\ \operatorname{div} \boldsymbol{\sigma}(\boldsymbol{x},t) = 0, \quad \boldsymbol{\sigma}(\boldsymbol{x},t)\cdot\boldsymbol{n}(\boldsymbol{x}) \text{ antiperiodic on } \partial V, \\ \boldsymbol{\varepsilon}(\boldsymbol{x},t) = \overline{\boldsymbol{\varepsilon}}(t) + \tfrac{1}{2}(\boldsymbol{\nabla} \boldsymbol{u}^*(\boldsymbol{x},t) + \boldsymbol{\nabla} \boldsymbol{u}^{*T}(\boldsymbol{x},t)),\ \boldsymbol{u}^*(\boldsymbol{x},t) \text{ periodic on } \partial V. \end{array}\right\} \quad (3)$$

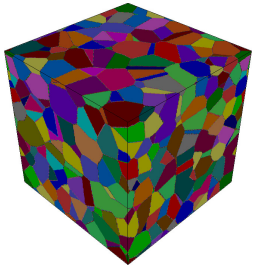

RVE V

$$\dot{\gamma}_s^{\mathsf{vp}} = \frac{\partial \psi_{\mathsf{vp},s}}{\partial \mathcal{A}_{\mathsf{vp},s}}\left(\mathcal{A}_{\mathsf{vp},s}, \mathcal{A}_{\mathsf{p},i}\right), \quad \dot{\gamma}_s^{\mathsf{p}} = \frac{\partial \psi_{\mathsf{p},s}}{\partial \mathcal{A}_{\mathsf{p},i}}\left(\mathcal{A}_{\mathsf{vp},s}, \mathcal{A}_{\mathsf{p},i}\right),\ s \in S_i,$$

with:
- $\boldsymbol{\varepsilon}_{\mathsf{vp}}$ associated with its thermodynamic force $\boldsymbol{\mathcal{A}}_{\mathsf{vp}} (\equiv \boldsymbol{\sigma})$,
- $p = (p_i)$ associated with its thermodynamic force $\mathcal{A}_{\mathsf{p}} = (\mathcal{A}_{\mathsf{p},i})$,
- $i \in \{\{100\},\{110\}\}$ referring to a slip family of the studied material [**Soulacroix**, *PhD Thesis* (2014)],

(4)

$$\mathcal{A}_{\mathsf{p},i}(\boldsymbol{x},t) = -r_i(\boldsymbol{x},t),$$
$$r_i(\boldsymbol{x},t) = \tau_i^0(T,\dot{\bar{\varepsilon}}) + h_i(T,\dot{\bar{\varepsilon}}) \times p_i(\boldsymbol{x},t),$$
$$\dot{p}_i = \sum_{s\in S_i} \dot{\gamma}_s^{\mathsf{p}}\left(\boldsymbol{\mathcal{A}}_{\mathsf{vp}}, \mathcal{A}_{\mathsf{p}}\right),\ \dot{\gamma}_s^{\mathsf{p}} = |\dot{\gamma}_s^{\mathsf{vp}}|.$$

Table of contents

Calibration of $\tau_i^0(T,\dot{\bar{\varepsilon}})$

$$n_{\{100\}} = 4,\ \dot{\gamma}^0_{\{100\}}(\dot{\bar{\varepsilon}}) = 0.7 \times \dot{\bar{\varepsilon}} \text{ and } n_{\{110\}} = 4,\ \dot{\gamma}^0_{\{110\}}(\dot{\bar{\varepsilon}}) = 0.5 \times \dot{\bar{\varepsilon}},$$

with:
- n_i deduced from observations,
- $\dot{\gamma}_i^0(\dot{\bar{\varepsilon}})$ determined using numerical tests at the single crystal scale.

$$\tau_i^0(T,\dot{\bar{\varepsilon}}) = A_i^{\mathsf{f}}(\dot{\bar{\varepsilon}}) \times exp\left(-b_i^{\mathsf{f}} \times T\right) + C_i^{\mathsf{f}}(\dot{\bar{\varepsilon}})$$

$$A_i^{\mathsf{f}}(\dot{\bar{\varepsilon}}) = Max\left[a_i^{\mathsf{f},0} - a_i^{\mathsf{f},1} \times exp\left[-a_i^{\mathsf{f},2} \times log_{10}\left(\dot{\bar{\varepsilon}}\right)\right], 0\right],$$

with:
- $C_i^{\mathsf{f}}(\dot{\bar{\varepsilon}})$ same strain rate dependence as $A_i^{\mathsf{f}}(\dot{\bar{\varepsilon}})$,
- $(A_i^{\mathsf{f}}, b_i^{\mathsf{f}}, C_i^{\mathsf{f}})$ **obtained by minimising error using *LM* algorithm** [**Levenberg**, *QAM* (1944)] [**Marquardt**, *JSIAM* (1963)],
- $\tau_i^0(T,\dot{\bar{\varepsilon}})$ targeted function.

$$\tau_i^{0,(n+1)}(T,\dot{\bar{\varepsilon}}) = \tau_i^{0,(n)}(T,\dot{\bar{\varepsilon}}) + f_s \times {}^{(n)}\Delta\bar{\sigma}^{\mathsf{cr}}_{33}(T,\dot{\bar{\varepsilon}}),\ f_s = 0.5,$$

with:
- $\tau_i^{0,(n+1)}$ input data used in the *LM* algorithm,

$$Er^{(n)} = \frac{1}{N} \times \sum |{}^{(n)}\Delta\bar{\sigma}^{\mathsf{cr}}_{33}(T,\dot{\bar{\varepsilon}})|,\ |Er^{(n)} - Er^{(n-1)}| < \delta \times Er^{(n-1)},$$

with:
- ${}^{(n)}\Delta\bar{\sigma}^{\mathsf{cr}}_{33}(T,\dot{\bar{\varepsilon}})$ error at given loading conditions,
- $(Er^{(n)}, \delta(=10^{-3}))$ relative error and stopping criterion.

Beginning of the iterative process

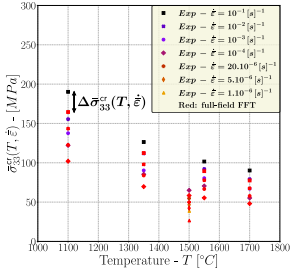

End of the iterative process

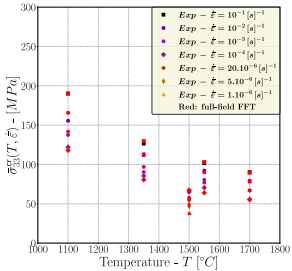

Calibration of $h_i(T, \dot{\bar{\varepsilon}})$

$$h_{\{100\}} = h_{\{110\}} = h$$

$$h^{(n+1)} = \frac{a_{\text{p,exp}} \times h^{(n)}}{a^{(n)}_{\text{p,simu}}},\ |a^{(n)}_{\text{p,simu}} - a_{\text{p,exp}}| < \delta \times a_{\text{p,exp}},$$

with:

- $a_{\text{p,exp}}$ experimental strain hardening slope,
- $a^{(n)}_{\text{p,simu}}$ numerical strain hardening slope,
- $\delta(= 10^{-4})$ relative stopping criterion.

$$h(T, \dot{\bar{\varepsilon}}) = \frac{a^{\text{h}} \times ln\left(b^{\text{h}} \times \dot{\bar{\varepsilon}} + f^{\text{h}}\right)}{\left(c^{\text{h}} \times T + d^{\text{h}}\right)^{e^{\text{h}}}},$$

with:

- $h^{(n)}$ input data used in the LM algorithm,
- $(a^{\text{h}}, b^{\text{h}}, c^{\text{h}}, d^{\text{h}}, e^{\text{h}}, f^{\text{h}})$ **coefficients determined by using *LM* algorithm** [**Levenberg**, *QAM* (1944)] [**Marquardt**, *JSIAM* (1963)].

(6)

End of the iterative process

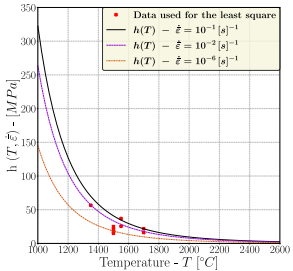

Results of Inverse Calibration

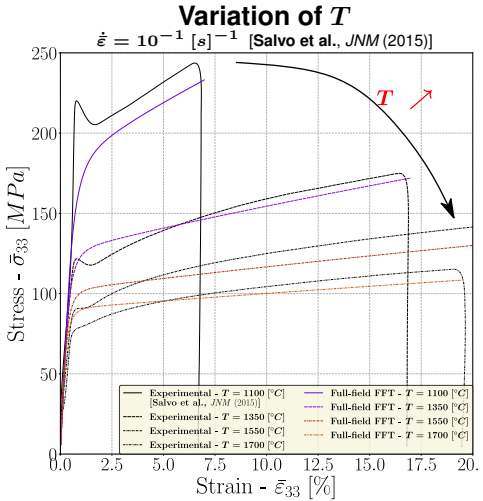

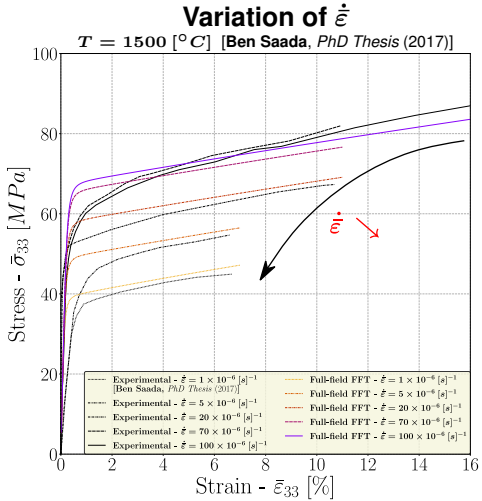

Table of contents

NTFA Decomposition of Internal Variables

$$\boldsymbol{\varepsilon}_{\mathsf{vp}}(\boldsymbol{x},t) = \sum_{k}^{M_{\mathsf{vp}}} \xi_{\mathsf{vp}}^{(k)}(t)\ \boldsymbol{\mu}_{\mathsf{vp}}^{(\boldsymbol{k})}(\boldsymbol{x}),$$

$\Big\|$ **NTFA decompostion** [**Michel and Suquet**, *JMPS* (2016)],

$$p_i(\boldsymbol{x},t) = \left| \begin{array}{l} \displaystyle\sum_{l}^{M_{\mathsf{p},i}} \xi_{\mathsf{p},i}^{(l)}(t)\ \mu_{\mathsf{p},i}^{(l)}(\boldsymbol{x}) \text{ - [Decomposed]}, \\ \displaystyle\sum_{g} \xi_{\mathsf{p},i}^{(g)}(t)\ \chi^{(g)}(\boldsymbol{x}) \text{ - [Constant per grain]}. \end{array} \right. \tag{7}$$

$\Big\|$ **[Constant per grain] - decomposition** [**Michel and Suquet**, *CM* (2016)],

$\Big\|$ **[Decomposed] - tested decomposition**,

with: $\left| \begin{array}{ll} \left(\boldsymbol{\mu}_{\mathsf{vp}}^{(\boldsymbol{k})}, \mu_{\mathsf{p},i}^{(l)}\right) & \text{modes used for the internal-variables decomposition,} \\ \left(\xi_{\mathsf{vp}},\ \xi_{\mathsf{p},i}\right) & \text{reduced internal variables.} \end{array} \right.$

Local Fields Expressed with Mode Decomposition

- $\boldsymbol{\varepsilon}(\boldsymbol{x},t) = \boldsymbol{A}(\boldsymbol{x}) : \bar{\boldsymbol{\varepsilon}}(t) + \sum_{l}^{M_{\text{vp}}} \boldsymbol{D} * \boldsymbol{\mu}_{\text{vp}}^{(\boldsymbol{l})}(\boldsymbol{x})\, \xi_{\text{vp}}^{(l)}(t),$

$\Big\|$ **induced by NTFA decompostion**,

with:

$\boldsymbol{\varepsilon}(\boldsymbol{x},t)$	using the superposition principle: solution to the linear thermoelastic problem[local problem (3)-(4)],
$\bar{\boldsymbol{\varepsilon}}$	macroscopic strain tensor,
$\boldsymbol{A}(\boldsymbol{x})$	strain concentration tensor,
$\boldsymbol{D} * \boldsymbol{\mu}_{\text{vp}}^{(\boldsymbol{l})}(\boldsymbol{x})$	strain influence tensor,

(8)

$$\boldsymbol{D} * \boldsymbol{\mu}_{\text{vp}}^{(\boldsymbol{l})}(\boldsymbol{x}) = \frac{1}{|V|}\int_{V} \boldsymbol{D}(\boldsymbol{x},\boldsymbol{x'}) : \boldsymbol{\mu}_{\text{vp}}^{(\boldsymbol{l})}(\boldsymbol{x'})\,\mathrm{d}\boldsymbol{x'},\ \boldsymbol{D}(\boldsymbol{x},\boldsymbol{x'}) = \boldsymbol{\Gamma}(\boldsymbol{x},\boldsymbol{x'}) : \boldsymbol{L}(\boldsymbol{x'}),$$

with: $(\boldsymbol{D},\boldsymbol{\Gamma})$ nonlocal and nonlocal Green operators,

- $\boldsymbol{\sigma}(\boldsymbol{x},t) = \boldsymbol{L}(\boldsymbol{x}) : \boldsymbol{A}(\boldsymbol{x}) : \bar{\boldsymbol{\varepsilon}}(t) + \sum_{l}^{M_{\text{vp}}} \boldsymbol{\rho}_{\text{vp}}^{(\boldsymbol{l})}(\boldsymbol{x})\, \xi_{\text{vp}}^{(l)}(t),$

with: $\boldsymbol{\rho}_{\text{vp}}^{(\boldsymbol{k})}(\boldsymbol{x}) = \boldsymbol{L}(\boldsymbol{x}) : \left(\left(\boldsymbol{D} * \boldsymbol{\mu}_{\text{vp}}^{(\boldsymbol{k})}\right)(\boldsymbol{x}) - \boldsymbol{\mu}_{\text{vp}}^{(\boldsymbol{k})}(\boldsymbol{x})\right).$

Macroscopic State Law

$$
\begin{aligned}
&\frac{\partial \bar{w}}{\partial \bar{\boldsymbol{\varepsilon}}} = \bar{\boldsymbol{\sigma}},\ \bar{\boldsymbol{\sigma}} = \tilde{\boldsymbol{L}} : \bar{\boldsymbol{\varepsilon}} + \sum_{k}^{M_{\mathsf{vp}}} < \boldsymbol{\rho}_{\mathsf{vp}}^{(\boldsymbol{k})} > \xi_{\mathsf{vp}}^{(l)},\\
-&\frac{\partial \bar{w}}{\partial \xi_{\mathsf{vp}}^{(k)}} = a_{\mathsf{vp}}^{(k)},\ a_{\mathsf{vp}}^{(k)} = \bar{\boldsymbol{\varepsilon}} : \boldsymbol{a}^{(\boldsymbol{k})} + \sum_{l} < \boldsymbol{\mu}_{\mathsf{vp}}^{(\boldsymbol{k})} : \boldsymbol{\rho}_{\mathsf{vp}}^{(\boldsymbol{l})} > \xi_{\mathsf{vp}}^{(l)},\\
-&\frac{\partial \bar{w}}{\partial \xi_{\mathsf{p},i}^{(k)}} = a_{\mathsf{p},i}^{(k)},\ a_{\mathsf{p},i}^{(k)} = \left| \begin{array}{l} -\left(\tau_i^0 < \mu_{\mathsf{p}_i}^{(k)} > + h_i \times \sum_{l}^{M_{\mathsf{p},i}} \xi_{\mathsf{p}_i}^{(l)} < \mu_{\mathsf{p}_i}^{(k)} \mu_{\mathsf{p}_i}^{(l)} > \right) \textbf{ - [Decomposed]},\\ -\left(\tau_i^0 + h_i \times \xi_{\mathsf{p}_i}^{(k)} \right) \times c^{(k)} \textbf{ - [Constant per grain]}, \end{array} \right.
\end{aligned}
\tag{9}
$$

with: $\left| \begin{array}{ll} \boldsymbol{a}^{(\boldsymbol{k})} & = < \boldsymbol{\mu}_{\mathsf{vp}}^{(\boldsymbol{k})} : \boldsymbol{L} : \boldsymbol{A} >, \\ \tilde{\boldsymbol{L}} & = < \boldsymbol{L} : \boldsymbol{A} > . \end{array} \right.$

Evolution of the Reduced Thermodynamic Variables

$$\dot{a}_{\mathsf{vp}}^{(k)}(\bar{\boldsymbol{\varepsilon}},\xi_{\mathsf{vp}}) = \frac{\partial a_{\mathsf{vp}}^{(k)}}{\partial \bar{\boldsymbol{\varepsilon}}} : \dot{\bar{\boldsymbol{\varepsilon}}} + \sum_{l}^{M_{\mathsf{vp}}} \frac{\partial a_{\mathsf{vp}}^{(k)}}{\partial \xi_{\mathsf{vp}}^{(l)}} \times \dot{\xi}_{\mathsf{vp}}^{(l)}, \text{ with } \dot{\xi}_{\mathsf{vp}}^{(l)} = \frac{\partial \psi_{\mathsf{vp}}^{\mathsf{hom}}}{\partial a_{\mathsf{vp}}^{(l)}} \Longrightarrow \dot{a}_{\mathsf{vp}}^{(k)} = \frac{\partial a_{\mathsf{vp}}^{(k)}}{\partial \bar{\boldsymbol{\varepsilon}}} : \dot{\bar{\boldsymbol{\varepsilon}}} + \frac{\partial \psi_{\mathsf{vp}}^{\mathsf{hom}}}{\partial \xi_{\mathsf{vp}}^{(k)}},$$

$$\psi^{\mathsf{hom}} = \tilde{\psi},\ \tilde{\psi} = <\psi>,\ <\psi> = \sum_{g} c^{(g)} \sum_{s} <\psi_s>^{(g)},$$

$\Big\|$ **approximation of the effective dissipation potential** [**Fritzen and Leuschner**, *CMAME* (2013)],

$$<\psi_{\mathsf{vp},s}^{\mathsf{TSO}}(\mathcal{A}_{\mathsf{vp},s},\mathcal{A}_{\mathsf{p},i})>^{(g)} = \Bigg[\psi_{\mathsf{vp},s}(\bar{\mathcal{A}}_{\mathsf{vp},s}^{(g)},\bar{\mathcal{A}}_{\mathsf{p},i}^{(g)}) + \frac{\partial^2 \psi_{\mathsf{vp},s}}{\partial \mathcal{A}_{\mathsf{vp},s}\partial \mathcal{A}_{\mathsf{p},i}} \times C^{(g)}\left(\mathcal{A}_{\mathsf{vp},s}^{(g)},\mathcal{A}_{\mathsf{p},i}^{(g)}\right)$$

$$+\frac{1}{2}\frac{\partial^2 \psi_{\mathsf{vp},s}}{\partial \mathcal{A}_{\mathsf{vp},s}^2} \times C^{(g)}\left(\mathcal{A}_{\mathsf{vp},s}^{(g)}\right) + \frac{1}{2}\frac{\partial^2 \psi_{\mathsf{vp},s}}{\partial \mathcal{A}_{\mathsf{p},i}^2} \times C^{(g)}\left(\mathcal{A}_{\mathsf{p},i}^{(g)}\right)\Bigg] \text{ - [Decomposed]}, \tag{10}$$

$\Big\|$ **Tangent Second Order (TSO) linearisation of the effective dissipation potential** [**Castañeda**, *JMPS* (1996)] [**Michel and Suquet**, *CM* (2016)].

with:
$$\begin{cases} C^{(g)}(X,Y) &= <\left(X-\bar{X}^{(g)}\right)\left(Y-\bar{Y}^{(g)}\right)>^{(g)}, \\ C^{(g)}(X) &= <\left(X-\bar{X}^{(g)}\right)^2>^{(g)}. \end{cases}$$

- **Similar work has to be done on $\dot{a}_{\mathsf{p}}^{(k)}$, $\dot{\boldsymbol{a}}_{\mathsf{vp}}^{(\boldsymbol{k})}$ has to be coupled with $\dot{a}_{\mathsf{p}}^{(k)}$.**

Table of contents

Uniaxial Compressive Strain Test: Macroscopic Comparison between Experimental Results, Full-Field FFT and NTFA-TSO Model

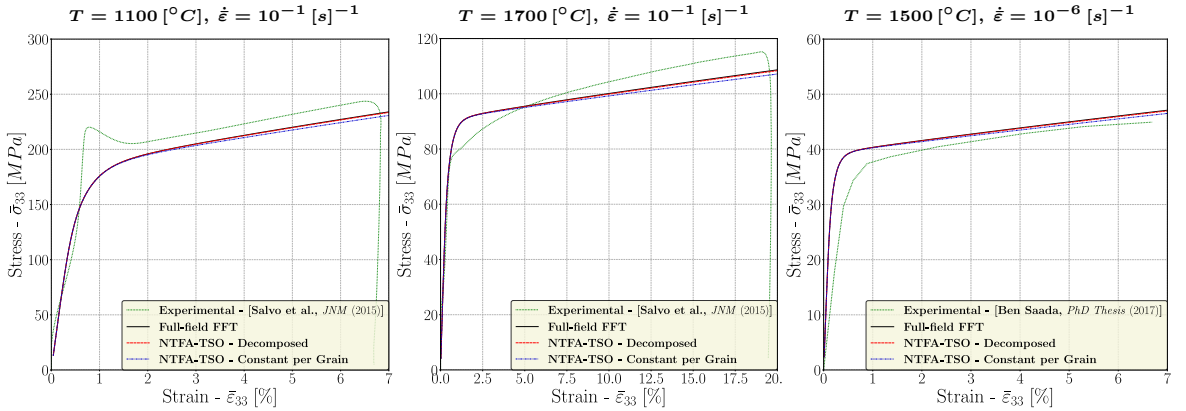

Uniaxial Compressive Strain Test: Local Comparison between Full-Field FFT and NTFA-TSO Model

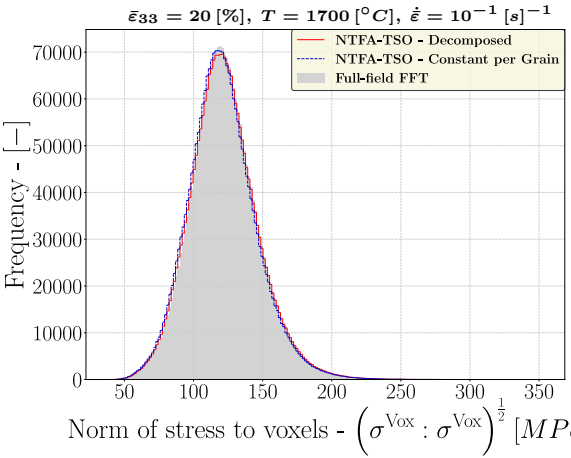

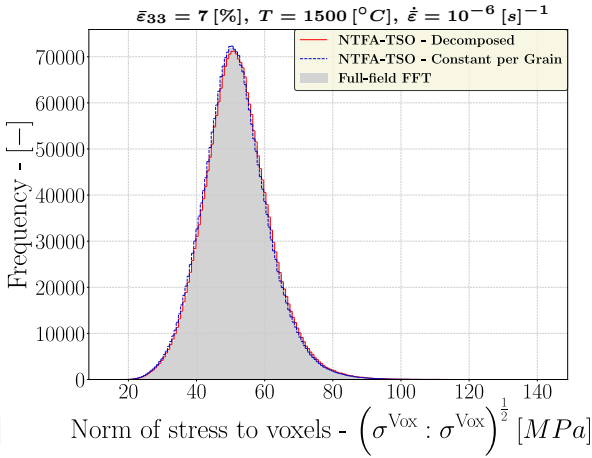

Conclusion

Mechanical problem

- ◇ Behaviour law $\Longleftarrow$ from experimental results
- ◇ Aim: to recover asymptotic behaviour

Inverse calibration

- ◇ Behaviour law parameters impacted by the loading conditions
- ◇ Iterative calibration process using Levenberg Marquardt algorithm

Model reduction: NTFA-TSO

- ◇ NTFA: 2 different decompositions studied
- ◇ Reduced-variable evolution laws $\Longleftarrow$ effective-dissipation-potential linearisation

Results

- ◇ **[Macroscopic scale]** Good agreement between:
  - Experimental results • FFT results • NTFA-TSO model
- ◇ **[Local scale]** Almost no error margin between: • FFT results • NTFA-TSO model

Perspectives

Objectives:

◇ To adapt the **NTFA-TSO model** to **all loading conditions** (RIA)

◇ To keep a **low number of internal variables**

Method: definition of reference loading conditions

◇ Temperature: $T_0 \in [|1000,\ 2600|]\,[^\circ C]$ with $T_{\text{Pas}} = 50\,[^\circ C]$

◇ Macroscopic strain rate: $\dot{\bar{\varepsilon}}_0 = 10^{-1}\,[s]^{-1}$

Future work:

◇ $[\boldsymbol{A}]$ Focus on temperature loading conditions

- ▶ 1D Lagrange interpolation functions on modes: $\boldsymbol{\mu}_{\text{vp}}(\boldsymbol{T_0})$

◇ $[\boldsymbol{B}]$ Focus on macroscopic strain rate loading conditions

- ▶ Same modes at $(\boldsymbol{T_0}, \dot{\bar{\boldsymbol{\varepsilon}}}_{\boldsymbol{0}})$ and $(\boldsymbol{T}, \dot{\bar{\boldsymbol{\varepsilon}}})$: $\boldsymbol{\mu}_{\text{vp}}(\boldsymbol{T}, \dot{\bar{\boldsymbol{\varepsilon}}})$
- ▶ Function: $T_0 = g_{|\dot{\bar{\varepsilon}}_0}(T, \dot{\bar{\varepsilon}})$
- ▶ Macroscopic strain rate domain: $\dot{\bar{\varepsilon}} \in [10^{-6},\ 10^{-1}]\,[s]^{-1}$

◇ $[\boldsymbol{C}]$ Developing a tri-axial loading NTFA-TSO model